

# Electrochemical evaluation and modification of commercial lithium cobalt oxide powders

J. Zhang, Y.J. Xiang, Y. Yu, S. Xie, G.S. Jiang, C.H. Chen\*

*Department of Materials Science and Engineering, University of Science and Technology of China, Anhui Hefei 230026, China*

Received 15 October 2003; received in revised form 5 January 2004; accepted 16 January 2004

## Abstract

As the cathode materials for rechargeable lithium batteries, five commercial lithium cobalt oxide powders have been investigated for a comparative study. The X-ray diffraction analysis indicates that all these powders exhibit the  $\alpha$ -NaFeO<sub>2</sub> layered structure. The size distribution and morphology were analyzed by particle sedimentation method and scanning electron microscopy (SEM). Their electrochemical properties including cycleability and especially 3.6 V plateau efficiency, a recently required control parameter, are compared. Two kinds of modifications, i.e. Li<sub>2</sub>CO<sub>3</sub> coating and high-temperature treatment, have been applied to improve the electrochemical performance of one of these five powders. After the high-temperature treatment in air, cobalt oxidation-state becomes higher and Li(Li<sub>x</sub>Co<sub>1-x</sub>)O<sub>2</sub> is formed. Both of the two modified means can significantly improve the 3.6 V-plateau efficiency through suppressing the cell impedance rise during cycling. A general discussion on the factors influencing the plateau efficiency is also given.

© 2004 Published by Elsevier B.V.

*Keywords:* Lithium cobalt oxide; Cellular phone; Modification; Plateau efficiency; Oxidation state

## 1. Introduction

In the first commercialized lithium ion battery from Sony Corporation in 1990, lithium cobalt oxide (LiCoO<sub>2</sub>) versus carbonaceous material was the main component of cell chemistry [1]. After two decades of researches and development, other cathode materials such as LiMn<sub>2</sub>O<sub>4</sub> [2–4] and LiNi<sub>1-x</sub>Co<sub>x</sub>O<sub>2</sub> [5–7] have been also identified as practical 4-V cathode materials for lithium secondary batteries. Although LiCoO<sub>2</sub> has drawbacks in cost and safety, it is advantageous compared with LiMn<sub>2</sub>O<sub>4</sub> and LiNi<sub>1-x</sub>Co<sub>x</sub>O<sub>2</sub> because of its easy synthesis and excellent cycleability. Moreover, in the voltage range between 4.2 and 3.6 V, LiCoO<sub>2</sub> shows a 1C-rate specific capacity of about 140 mAh/g, that is comparable to that of LiNi<sub>1-x</sub>Co<sub>x</sub>O<sub>2</sub> but higher than that of LiMn<sub>2</sub>O<sub>4</sub>. Therefore, currently LiCoO<sub>2</sub> remains to dominate the market of cathode materials, especially for the batteries of cellular phones. Various R&D efforts continue to be made to further improve the performance of LiCoO<sub>2</sub>. These efforts include new synthesis routes [8,9], aluminum doping [10–12], and coating the LiCoO<sub>2</sub> particles with Al<sub>2</sub>O<sub>3</sub> [13] or MgO [14]. On the

other hand, the quality of LiCoO<sub>2</sub> powdered product from different manufacturers varies a lot due to their different synthesis procedures and conditions. This quality difference leads to different life time of lithium-ion batteries of cellular phones; some LiCoO<sub>2</sub>/C cells can only be effectively rechargeable for about 100 times, whereas others for 300–500 times. It is hence necessary to compare LiCoO<sub>2</sub> powders from different manufactures and investigate the origin of their difference in electrochemical properties.

Recently, the cellular phone industry in China placed a new control parameter called “plateau efficiency” on the quality of cathode materials. The plateau efficiency ( $\eta_E$ ) of a cell may be defined as  $\eta_E = Q_E/Q_{tot}$ , where  $Q_E$  is the dischargeable 1C-rate capacity from its fully charged state to a certain voltage  $E$ , and  $Q_{tot}$  is its total 1C-rate capacity. Therefore,  $\eta_E$  is also equal to the depth-of-discharge (DOD) at the voltage  $E$ . For LiCoO<sub>2</sub>, this required control parameter is currently  $\eta_{3.6V}$ , i.e. the ratio of the capacity from 4.2 to 3.6 V over the capacity from 4.2 to 2.8 V. To our knowledge, study on the change of the plateau efficiency with battery cycling has not been reported in literature.

Therefore, the comparison of commercial LiCoO<sub>2</sub> powders from selected manufacturers and exploration of ways to improve these powders provided the motivation for this study. A special attention was paid to the plateau efficiency as a critical parameter in the comparison. First we evaluated

\* Corresponding author. Tel.: +86-551-3602938;  
fax: +86-551-3602940.  
E-mail address: [cchchen@ustc.edu.cn](mailto:cchchen@ustc.edu.cn) (C.H. Chen).

five commercial  $\text{LiCoO}_2$  powders in terms of the crystalline structure, particle morphology, and electrochemical properties including the plateau efficiency. Then we took two approaches, i.e. second-time high temperature firing and  $\text{Li}_2\text{CO}_3$  coating, to modify one of these commercial  $\text{LiCoO}_2$  powders. After the modifications, its electrochemical properties have been markedly improved.

## 2. Experimental aspects

### 2.1. Commercial $\text{LiCoO}_2$ powders and treatment

Five commercial  $\text{LiCoO}_2$  powders were obtained from different manufacturers, three from Mainland China, one from Taiwan and one from Japan. They were coded in this study as CoA, CoB, CoC, CoD, and CoE, respectively. All of them were synthesized by a solid-state reaction from  $\text{Li}_2\text{CO}_3$  and  $\text{Co}_3\text{O}_4$ . These as-received powders were made into electrode laminates (see below) for evaluation study. In addition, the pristine  $\text{LiCoO}_2$  powder from Dalian (CoE) was modified by two techniques. In the first modification, the powder was soaked in a mixed aqueous solution of 1 M  $\text{LiOH}$  and 0.25 M  $\text{LiNO}_3$  for 30 min, then filtered out and dried up. The filtered  $\text{LiCoO}_2$  powder was kept at  $250^\circ\text{C}$  in  $\text{CO}_2$  for 4 h in order to form a  $\text{Li}_2\text{CO}_3$  coating on the powder particles. This coated powder was coded as CoE2. In the second modification, CoE powder was modified with two parallel second-time firing, one at  $850^\circ\text{C}$  in air for 8 h and another at  $1000^\circ\text{C}$  in air for 7 h. The resulted  $\text{LiCoO}_2$  powders were coded as CoE3 and CoE4, respectively.

### 2.2. Structural and compositional analyses

The crystal structure of the powders was analyzed using X-ray diffraction (Rigaku D/Max-rA,  $\text{Cu K}\alpha$  radiation). The scanned range was from  $15$  to  $75^\circ$  ( $2\theta$ ). Their particle morphology was studied using a scanning electron microscope (KYKY-AMRAY 1000 B). The particle size distribution was measured with a sedimentation-type photo size analyzer (NSKC-1A).

The average oxidation-state of cobalt in  $\text{LiCoO}_2$  samples was determined by the iodometry. In this analysis,  $\text{LiCoO}_2$  was first dissolved in a dilute hydrochloric aqua solution. The reduction of  $\text{Co}^{4+}$  and  $\text{Co}^{3+}$  to  $\text{Co}^{2+}$  was achieved by adding  $\text{I}^-$  into the solution, forming  $\text{I}_3^-$ . Back titration for the resulting  $\text{I}_3^-$  was carried out by a  $\text{Na}_2\text{S}_2\text{O}_3$  solution with a predetermined concentration.

### 2.3. Electrode preparation and electrochemical measurements

The electrode laminate for the electrochemical testing was prepared by casting a slurry consisting of active material powders (84 wt.%), acetylene black (8 wt.%), and poly(vinylidene fluoride) (PVDF) (8 wt.%) dispersed in

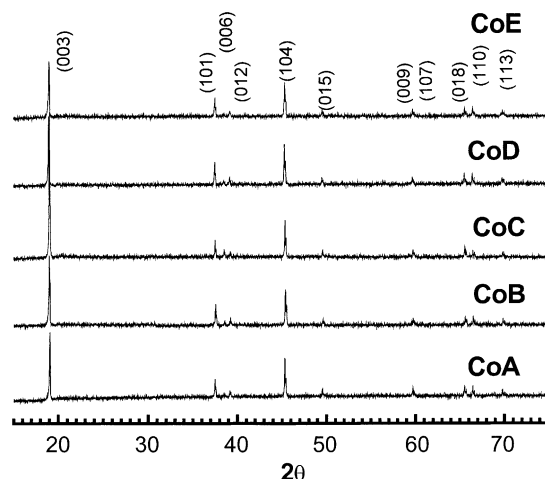


Fig. 1. XRD patterns of five commercial  $\text{LiCoO}_2$  powder samples.

1-methyl-2-pyrrolidinone (NMP) onto an aluminum foil. The laminates were then dried at  $70^\circ\text{C}$  for 2 h and calcined to obtain an electrode porosity between 65 and 70%.

$\text{LiCoO}_2/\text{Li}$  coin-cells (2032 size) were made with 1 M  $\text{LiPF}_6$  in ethylene carbonate (EC): diethyl carbonate (DEC) (1:1 (w/w)) as the electrolyte. The cells were tested on a multi-channel battery cyler (Shenzhen Neware Co. Ltd.). In the first three cycles, a constant current density of  $0.20\text{ mA/cm}^2$  was applied in the voltage range between 4.2 and 2.8 V. Then the current was increased to 1C-rate. AC impedance spectra of some charged cells were measured with an electrochemical workstation (CHI 604A).

## 3. Results and discussion

### 3.1. Structure and electrochemical valuation of pristine commercial $\text{LiCoO}_2$ powders

#### 3.1.1. Crystalline structure of five $\text{LiCoO}_2$ powders

It can be seen from the XRD patterns Fig. 1 that all of the original  $\text{LiCoO}_2$  powders exhibit pure-phase  $\alpha\text{-NaFeO}_2$  layered structure. Since well-defined peak doublets (006, 012) and (018, 110) appear in these patterns, it is an indication of the stabilization of the two-dimensional structure and an ordered distribution of lithium and cobalt ions in the lattice [15]. Table 1 lists the lattice parameters determined

Table 1  
The lattice parameters and crystallite size of commercial  $\text{LiCoO}_2$  powders

Sample	$a$ (Å)	$c$ (Å)	$c/a$	Crystallite size ( $\mu\text{m}$ )
CoA	2.812	13.980	4.972	7.3
CoB	2.812	13.980	4.971	6.8
CoC	2.846	13.976	4.911	7.1
CoD	2.850	14.023	4.920	7.0
CoE	2.847	14.006	4.920	6.4

by the least-squares refinement of peak positions, average crystallite size calculated by the Scherrer equation [16] and tap density of the pristine powders. Obviously, the  $c/a$  ratio of CoA and CoB powders is significantly greater than the ideal  $c/a$  ratio of 4.899 for cubic-close-packed structure, while that of other powders is close to 4.899. In addition, the average crystallite size is all from 6 to 8  $\mu\text{m}$ , meaning the powders are consisted of single crystal grains of this size. Nevertheless, the crystallite size obtained from XRD measurement is usually not very accurate and should only be treated accurate enough in terms of its order of magnitude.

### 3.1.2. Morphology and particle size distribution of five $\text{LiCoO}_2$ powders

Generally speaking, the desirable particle morphology of an electrode powder is a trade-off result of many factors including surface area, tap density and electrical conductivity. Smaller particles can favorably facilitate the ionic conduction in the electrode due to a shorter distance of lithium diffusion from the surface to the core of the particles, but the increased surface area may unfavorably lead to more unwanted side reactions at the interface between the liquid electrolyte and electrode. Also, too small particles may result in a low tap density, and thus, reduce the

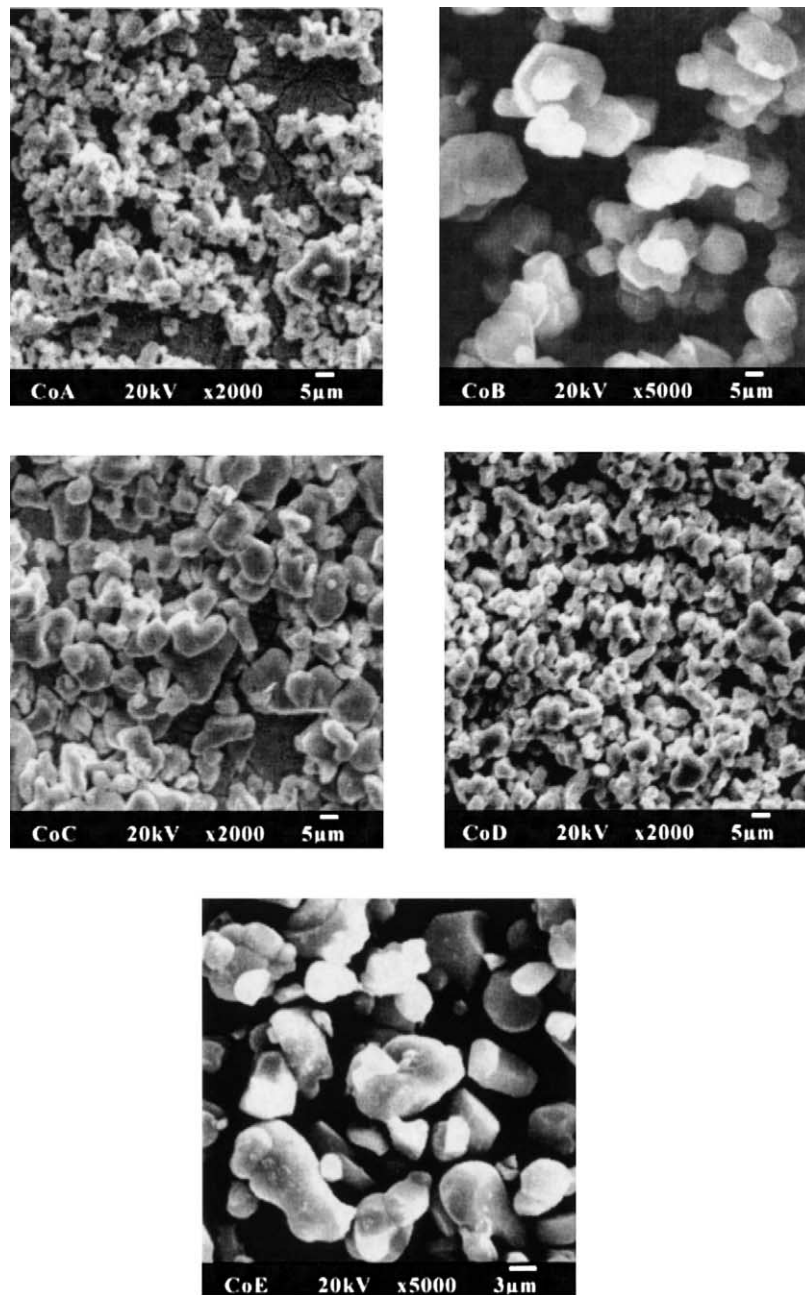


Fig. 2. The SEM micrographs of five commercial  $\text{LiCoO}_2$  samples.

Table 2  
Particle size distribution and tap density of five pristine and three treated LiCoO<sub>2</sub> powders

Samples	Particle size (μm)			Tap density (g/cm <sup>3</sup> )
	D10	D50	D90	
CoA	3.4	7.4	22	2.2
CoB	4.4	9.2	22	2.4
CoC	4.1	9.2	23	2.2
CoD	2.2	5.0	13	2.1
CoE	2.4	5.7	21	2.4
CoE2	2.5	5.8	23	–
CoE3	3.3	5.9	10	–
CoE4	3.1	6.4	11	–

volumetric energy density of the cell made with this electrode powder. According to many manufacturers for cellular phone lithium-ion batteries, the favorable particle size of LiCoO<sub>2</sub> powders should be between 2 and 10 μm. Fig. 2 shows the scanning electron microscopy (SEM) images of the five commercial powders, while the measurement results of particle size distributions of the five commercial powders are listed in Table 2. It is observed that all of these powders have suitable particle size range. Nevertheless, CoA is quite different from the other powders in that it is composed of rather irregular particles with a broad particle size distribution. CoB and CoC have the similar particle size distribution and the median size D50 (about 9.2 μm). It is believed a LiCoO<sub>2</sub> powder with a narrower particle size distribution around 5–7 μm is optimal to achieve a better electrochemical performance. Therefore, CoD has the most optimal size distribution among all powders. For CoE, it shows a broader particle size distribution than CoD although its median size (5.7 μm) is in the optimal range. Hence, the electrochemical property of CoE should be worse than that of CoD if only considering the morphological aspect.

### 3.1.3. Electrochemical characterization

The plot of the discharge capacity of LiCoO<sub>2</sub>/Li cells as a function of cycle number for five commercial LiCoO<sub>2</sub> powders is shown in Fig. 3. Note that the capacity of first three cycles was measured at 0.2 mA/cm<sup>2</sup> (equivalent C/5 to C/7 rate) while the subsequent cycles were conducted at 1C-rate. For all of the five LiCoO<sub>2</sub> powders, the first charge capacity is found in the range of 140–150 mAh/g, while the first discharge capacity is about 135–145 mAh/g. This initial capacity loss is ascribed to the passivation reaction either on the surface of the cathode or on that of the lithium anode. Furthermore, the discharge–charge efficiency is nearly 100% after the three formation cycles.

It can be seen from Fig. 3 that CoD shows better cycleability than other four commercial LiCoO<sub>2</sub> powders. After 100 1C-rate cycles, 92% of the capacity of CoD/Li cell is still retained, while the capacity of cells made with other LiCoO<sub>2</sub> powders has dropped to below 80% after 50 cycles. This is

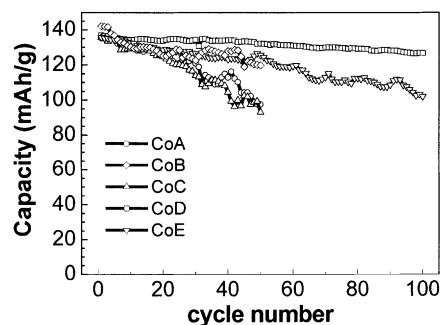


Fig. 3. Specific capacity as a function of cycle number for LiCoO<sub>2</sub>/Li cells. The LiCoO<sub>2</sub> electrodes were made from five commercial powders CoA, CoB, CoC, CoD, and CoE. The charge–discharge was operated in the voltage range between 4.2 and 2.8 V at the current density of 0.20 mA/cm<sup>2</sup> for first three cycles and 1.0–1.4 mA/cm<sup>2</sup> (or 1C-rate) for the subsequent cycles.

consistent with above results of morphological analysis of these LiCoO<sub>2</sub> powders. Therefore, the average particle size and its distribution play a significant role in the cycling performance. The LiCoO<sub>2</sub> powder with regular spherical particles and a narrow size distribution, i.e. CoD, is more stable against volume changes during intercalation/de-intercalation than those comprising of smaller crystallites, such as CoA and CoE, and those having a broad particle size distribution, such as CoB and CoC.

Fig. 4 shows the plateau efficiency  $\eta_{3.6V}$  of LiCoO<sub>2</sub>/Li cells as a function of cycleability. Comparing Figs. 3 and 4, one can see that the degradation of plateau efficiency does not keep the same pace of the capacity fading. A cell with poor capacity retention must be one with poor stability of its plateau efficiency. This is the case for the CoA/Li, CoB/Li or CoC/Li cells. On the other hand, a cell with good capacity retention does not necessarily warrant good stability of the plateau efficiency. This is the case for the CoE/Li cell. Only the CoD/Li cell exhibits both good capacity retention and good stability of plateau efficiency. Therefore, the plateau efficiency is a stricter control parameter than the capacity retention to evaluate the quality of electrode materials for lithium-ion cells.

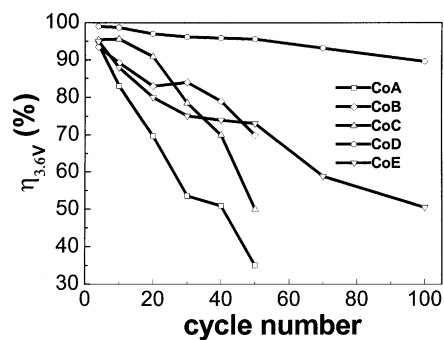


Fig. 4. The plateau efficiency  $\eta_{3.6V}$  of LiCoO<sub>2</sub>/Li cells. The testing conditions are given in the caption of Fig. 3.

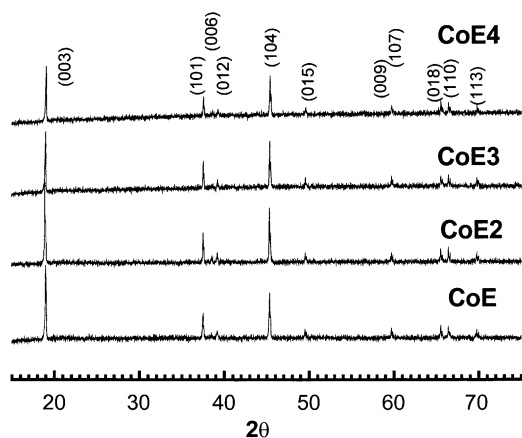


Fig. 5. XRD patterns of the sample CoE before and after retreatment.

### 3.2. Structure and electrochemical property of modified $\text{LiCoO}_2$ powders

#### 3.2.1. Crystalline structure of modified $\text{LiCoO}_2$ powders

Fig. 5 shows the XRD patterns of treated CoE– $\text{LiCoO}_2$  powders. The intensity ratio of  $I(003)/I(104)$  and Co oxidation state determined by the iodometry are listed in Table 3. It is observed that the intensity ratio of  $I(003)/I(104)$  decreases after the original powder CoE was treated at high temperatures. It seems that a higher treatment temperature leads to a smaller  $I(003)/I(104)$  ratio. According to the X-ray diffraction rule of  $\text{LiMO}_2$  ( $M = \text{Co}, \text{Ni}, \text{V}, \text{and Cr}$ ) with a rock-salt structure, the  $I(003)/I(104)$  ratio becomes reduced when either M ions partially occupies the octahedral sites of the lithium layer namely  $(\text{Li}_{1-x}\text{M}_x)\text{MO}_2$  or Li partially occupies the M-sites namely  $\text{Li}(\text{Li}_x\text{M}_{1-x})\text{O}_2$ . Whether the decrease of  $I(003)/I(104)$  ratio is due to  $(\text{Li}_{1-x}\text{M}_x)\text{MO}_2$  or  $\text{Li}(\text{Li}_x\text{M}_{1-x})\text{O}_2$  can be distinguished by determining if the oxidation state of the transition metal ion M is less or greater than 3. Because the iodometric titration result (Table 3) shows that Co oxidation states of CoE, CoE2, CoE3, and CoE4 are 3.01, 3.02, 3.11, and 3.13, respectively, the most likely scenario is  $\text{Li}(\text{Li}_x\text{Co}_{1-x})\text{O}_2$ . Considering the relatively high volatility of cobalt-component in many Co-containing ceramic oxides at high temperatures, this Co-deficient composition can be understood. Compared with CoE, CoE2 is only through a low temperature ( $250^\circ\text{C}$ ) heat treatment in addition to its surface coating at room temperature. Hence, its cobalt component should be hardly “evaporated” from CoE and consequently the oxidation-state of cobalt changes very little. This is

exactly observed in Table 3. CoE3 and CoE4 samples are from high-temperature treatment of CoE in air. Due to the “evaporation” of Co-component, metal ions rearrange their positions in the lattice structure so that lithium ions occupy Co-sites to form  $\text{Li}(\text{Li}_x\text{Co}_{1-x})\text{O}_2$ . The higher the treatment temperature, the greater  $x$  is. Therefore, the oxidation-state of Co in CoE4 is greater than CoE3. Assuming no oxygen defects in the structure, the amount of lithium ions that occupy Co-sites,  $x$ , can be calculated with the relationship  $x = (V - 3)/(V - 1)$ , where  $V$  is the oxidation-state of Co. Thus, it is 0.005, 0.01, 0.052, and 0.061 for CoE, CoE2, CoE3, and CoE4, respectively.

#### 3.2.2. Morphology and particle size distribution of treated $\text{LiCoO}_2$ powders

The scanning electron microscopy images of both original CoE and treated CoE powders are shown in Fig. 6. Basically, no significant difference in the particle morphology can be observed between the  $\text{LiCoO}_2$  powders before and after treatment. Specifically, there is no direct evidence to view the presence of  $\text{Li}_2\text{CO}_3$  coating in CoE2, which is also not detected by XRD (Fig. 5). Nevertheless, the treatment procedure and the improvement of the electrochemical property (see below) reveal a high likelihood for the presence of a very thin  $\text{Li}_2\text{CO}_3$  surface coating. As for CoE3 and CoE4, their particle size distribution becomes narrower after high-temperature treatment (Table 2). Probably, those particles with a small size for instance below  $2\ \mu\text{m}$  have grown bigger during the second-time sintering at high temperatures ( $850$  and  $1000^\circ\text{C}$ ). On the other hand, the big particles above  $15\ \mu\text{m}$  in size in CoE are mostly agglomerates (Fig. 2) and can be de-agglomerated during the grinding of treated powders. As a result of above two factors, the particle size distribution of CoE3 and CoE4 becomes narrower with almost unchanged D50 compared to their original powder CoE.

#### 3.2.3. Electrochemical characterization of treated $\text{LiCoO}_2$ powders

Figs. 7–9 show the plots of voltage profiles, the specific capacity, and the 3.6 V-plateau efficiency as a function of cycle number for pristine-CoE and treated-CoE/Li cells. Apparently, the two kinds of treatments, i.e.  $\text{Li}_2\text{CO}_3$  coating and second-time sintering cause little changes in the initial capacity of  $\text{LiCoO}_2$  powders because the initial capacity of these cells is all measured to be 135–140 mAh/g, the differences of which are within the experimental error. Nevertheless, the treatments have slightly improved the plateau efficiency as the 3.6 V-plateau efficiency at the fourth cycle that is also the first 1C-rate cycle, is increased from 95 to about 97%. Furthermore, both  $\text{Li}_2\text{CO}_3$  coating and high-temperature treatment have also improved the cycleability of treated  $\text{LiCoO}_2$  powders including the capability of capacity retention (Fig. 8) and, more significantly, the stability of plateau efficiency (Fig. 9). Specifically, after 100 cycles the specific capacity of CoE/Li, CoE2/Li, CoE3/Li, and CoE4/Li cells has faded to 102, 117, 117,

Table 3  
Structure and Co oxidation state analysis of  $\text{LiCoO}_2$  powders

	CoE	CoE2	CoE3	CoE4
Intensity ratio of $I(003)/I(104)$	1.63	1.61	1.40	1.29
Co oxidation state	3.01	3.02	3.11	3.13
$x$ in $\text{Li}(\text{Li}_x\text{Co}_{1-x})\text{O}_2$	0.005	0.01	0.052	0.061

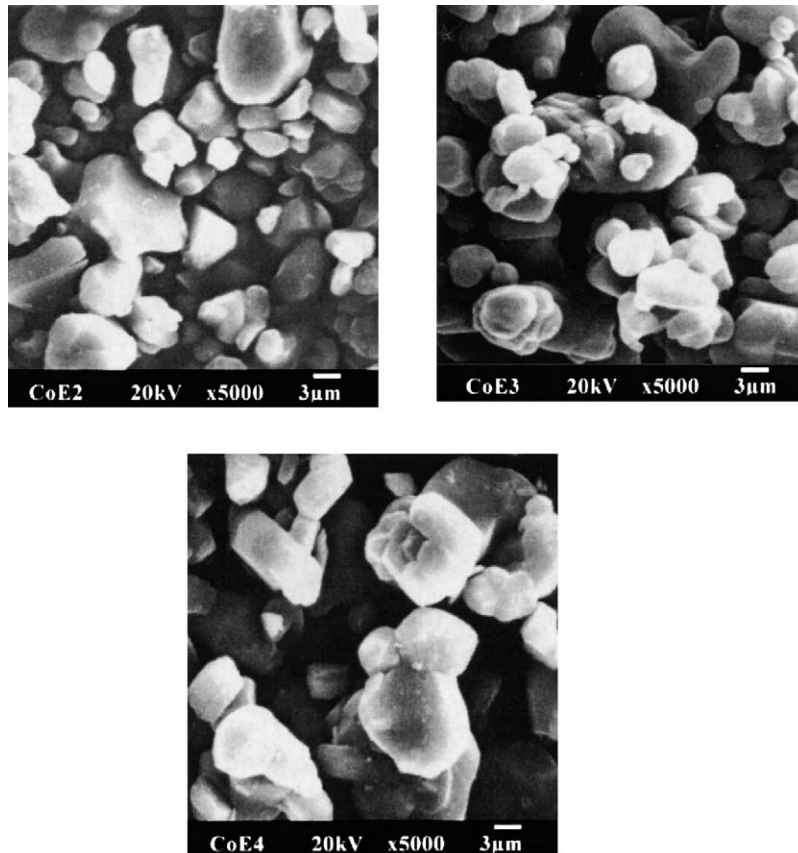


Fig. 6. The typical SEM micrographs of the original sample CoE and retreated samples, i.e. CoE2, CoE3, and CoE4, all micrographs with the magnification of 5000.

and 110 mAh/g, respectively; their 3.6 V-plateau efficiency has dropped to 50.5, 78.2, 78.4, and 71.2%, respectively. Therefore, the two treatments adopted in this study can effectively improve the performance of  $\text{LiCoO}_2$  powders as the active electrode material for rechargeable lithium batteries. Nevertheless, it is noticed (Figs. 8 and 9) that CoE4/Li cell performs not so well as CoE3/Li cell after 30 cycles. This difference might suggest that the heat-treatment temperature 1000 °C is too high for the modification. At this

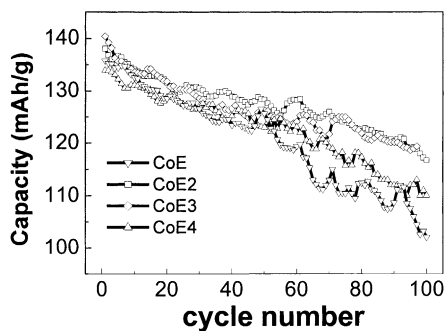


Fig. 7. The charge–discharge curves of  $\text{LiCoO}_2/\text{Li}$  cells. The  $\text{LiCoO}_2$  electrodes were made from CoE, CoE2, CoE3, and CoE4 powders. The charge–discharge was operated in the voltage range between 4.2 and 2.8 V at the current density of 0.20 mA/cm<sup>2</sup> for first three cycles and 1.0–1.4 mA/cm<sup>2</sup> (or 1C-rate) for the subsequent cycles.

high temperature, both lithium and cobalt may be partially lost, resulting in possibly small amount of impurity phases like  $\text{Co}_3\text{O}_4$  in the product.

The plateau efficiency of a cell should be intrinsically determined by two factors: (1) the nature of electrodes (including cathode and anode) materials, and (2) the cell impedance. The nature of an electrode material gives a certain feature of potential profile against metallic lithium. For example the potential profile of  $\text{LiCoO}_2$ , which is a so-called 4 V-electrode in nature [17], determines that nearly 100% of its potential during delithiation is above 3.6 V against Li.

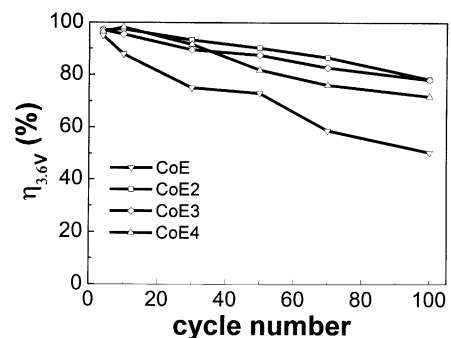


Fig. 8. Specific capacity as a function of cycle number for  $\text{LiCoO}_2/\text{Li}$  cells. The testing conditions are given in the caption of Fig. 7.

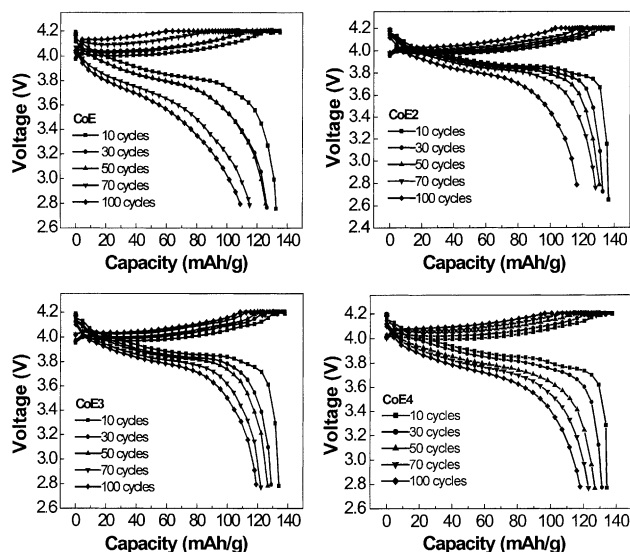


Fig. 9. The plateau efficiency  $\eta_{3.6V}$  of  $\text{LiCoO}_2/\text{Li}$  cells. The testing conditions are given in the caption of Fig. 7.

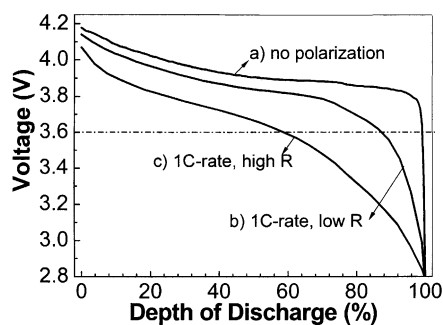


Fig. 10. The illustration of the plateau efficiency of a hypothetical  $\text{LiCoO}_2/\text{Li}$  cell.

Therefore, as illustrated by in Fig. 10 (curve a), if the polarization effect can be neglected, the 3.6 V-plateau efficiency of  $\text{LiCoO}_2$  should be close to 100%. This is exactly observed for almost all  $\text{LiCoO}_2/\text{Li}$  cells investigated in this study during their first three formation cycles under a small current density. On the other hand, the plateau efficiency is defined as a parameter obtained at 1C-rate current. The polarization of electrodes, which is not negligible at such a high rate,

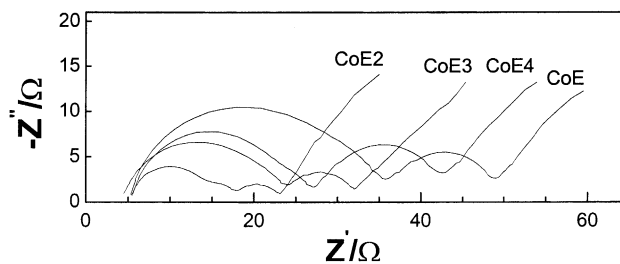


Fig. 12. AC impedance spectra of  $\text{CoE}/\text{Li}$ ,  $\text{CoE}_2/\text{Li}$ ,  $\text{CoE}_3/\text{Li}$ , and  $\text{CoE}_4/\text{Li}$  cells at open-circuit voltage 4.0 V after 50 electrochemical cycles. The cycling conditions are given in the caption of Fig. 7.

may be equivalent to ohmic  $IR$  drop, where  $I$  is the current passing the cell and  $R$  is the cell impedance. Owing to this  $IR$  drop, the discharge voltage profile is drawn downward (curves b and c in Fig. 10). Obviously, the extent of this downward shift is proportional to  $R$ . Therefore, the plateau efficiency is reduced with increasing  $R$ .

Usually, the cell impedance is largely contributed from the interfacial resistance between the  $\text{LiCoO}_2$  and the liquid electrolyte. As mentioned above, the  $\text{Li}_2\text{CO}_3$ -coating and high-temperature treatment only slightly increases the initial 3.6 V-plateau efficiency of  $\text{CoE}/\text{Li}$  cells from 95 to 97%. Very likely, the improvement by  $\text{Li}_2\text{CO}_3$  coating is originated from the reduction of the interfacial resistance. As for the improvement brought by the high-temperature treatment, it is related to the change of cathode composition. At the voltage of 3.6 V, the cathode composition in the  $\text{CoE}/\text{Li}$  cell is close to  $\text{LiCoO}_2$  where nearly all cobalt ions are  $\text{Co}^{3+}$ , which gives rise to a relatively low electronic conductivity, which is believed to dominate the interfacial resistance of a cell [18], and thus, a large total cell resistance  $R$ . On the other hand, the cathode composition in the  $\text{CoE}_3/\text{Li}$  and  $\text{CoE}_4/\text{Li}$  cells is close to  $\text{Li}(\text{Li}_x\text{Co}_{1-x})\text{O}_2$  (Table 3). This composition contains mixed  $\text{Co}^{3+}/\text{Co}^{4+}$  ions, which give rise to relatively high electronic conductivity and hence low  $R$ . Therefore, the improvement of initial plateau efficiency can be understood by the reduction of interfacial resistance at the voltage of 3.6 V.

During the cycling of  $\text{LiCoO}_2/\text{Li}$  cells, the cell impedance in particular the interfacial resistance increases continuously, as is shown in Fig. 11 for the  $\text{CoE}/\text{Li}$  cell. This increase

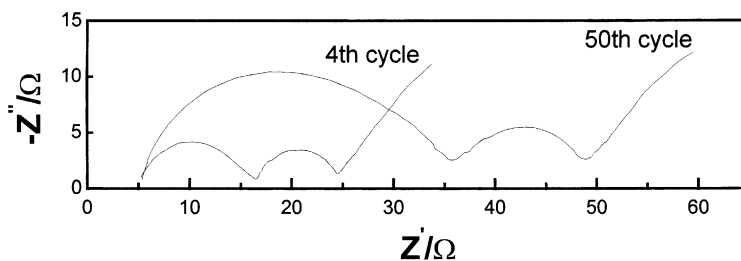


Fig. 11. AC impedance spectra of  $\text{CoE}/\text{Li}$  cells at open-circuit voltage 4.0 V after different electrochemical cycles. The cycling conditions are given in the caption of Fig. 7.

in the cell impedance causes the reduction of plateau efficiency (Fig. 9). Apparently, both  $\text{Li}_2\text{CO}_3$  coating and partial lithium substitution in Co-site, i.e.  $\text{Li}(\text{Li}_x\text{Co}_{1-x})\text{O}_2$ , exhibit the effect of suppressing the impedance rise during cycling of  $\text{LiCoO}_2/\text{Li}$  cells. This is also confirmed by the impedance measurement (Fig. 12).

#### 4. Conclusions

Five commercial  $\text{LiCoO}_2$  powders have been evaluated in terms of particle morphology, particle size distribution, crystalline structure, and electrochemical property especially 3.6 V-plateau efficiency. It is found that powders with a narrow size distribution and uniform spherical morphology exhibit optimal electrochemical properties. For one of these commercial powders, two kinds of modifications, i.e.  $\text{Li}_2\text{CO}_3$  coating and high-temperature treatment, have been applied to improve effectively the electrochemical performance especially the initial 3.6 V-plateau efficiency and its stability over cycling of cells.

#### Acknowledgements

This study was supported by 100 Talents Program of Academia Sinica and National Science Foundation of China (contract No. 50372064). The authors are also grateful to Mr. Xiangmu Shen from Haiyi Crystal Ltd. for providing commercial  $\text{LiCoO}_2$  powders.

#### References

- [1] Y.E. Hyung, S.I. Moon, D.H. Yum, S.K. Yun, *J. Power Sources* 82 (1999) 842.
- [2] J.J. Xu, J.S. Yang, *Electrochem. Commun.* 5 (2003) 23.
- [3] H.W. Chan, J.G. Duh, S.R. Sheen, *J. Power Sources* 115 (2003) 110.
- [4] R. Vacassy, H. Hofmann, N. Papageorgiou, M. Gratzel, *J. Power Sources* 81–82 (1999) 621.
- [5] S.P. Lin, K.Z. Fung, Y.M. Hon, M.H. Hon, *J. Crystal Growth* 226 (2001) 148.
- [6] J. Cho, G. Kim, H.S. Lim, *J. Electrochem. Soc.* 146 (10) (1999) 3751.
- [7] G.S. Rao, B.V.R. Chowdari, H.J. Lindner, *J. Power Sources* 97–98 (2001) 313.
- [8] Y.X. Li, C.R. Wan, Y.P. Wu, C.Y. Jiang, Y.J. Zhu, *J. Power Sources* 85 (2000) 294.
- [9] S.L. Rodrigues, N. Munichandraiah, A.K. Shukla, *J. Power Sources* 102 (2001) 322.
- [10] N. Amdouni, H. Zarrouk, F. Soulette, C. Julien, *Mater. Chem. Phys.* 80 (2003) 205.
- [11] G. Ceder, Y.-M. Chiang, D.R. Sadoway, M.K. Aydinol, Y.-I. Jang, B. Huang, *Nature* 392 (1998) 694.
- [12] W.S. Yoon, K.-K. Lee, K.-B. Kim, *J. Powder Sources* 97–98 (2001) 303.
- [13] Z.X. Wang, L.J. Liu, L.Q. Chen, X.J. Huang, *Solid State Ionics* 148 (2002) 335.
- [14] M. Mladenov, R. Stoyanova, E. Zhecheva, S. Vassilev, *Electrochem. Commun.* 3 (2001) 410.
- [15] S. Madhavi, G.V. Subba Rao, B.V.R. Chowdari, S.F.Y. Lia, *J. Electrochem. Soc.* 148 (2001) A1279.
- [16] C. Roth, M. Goetz, H. Fuess, *J. Appl. Electrochem.* 31 (7) (2001) 793.
- [17] Y. Ito, Y. Idemoto, Y. Tsunoda, N. Koura, *J. Power Sources* 119 (2003) 733.
- [18] F. Nobili, R. Tossici, F. Croce, B. Scrosati, R. Marassia, *J. Power Sources* 94 (2001) 238.